

**Hydrogen Activation**

International Edition: DOI: 10.1002/anie.201900861

German Edition: DOI: 10.1002/ange.201900861

**A New Mode of Chemical Reactivity for Metal-Free Hydrogen Activation by Lewis Acidic Boranes**

Elliot L. Bennett, Elliot J. Lawrence, Robin J. Blagg, Anna S. Mullen, Fraser MacMillan, Andreas W. Ehlers, Daniel J. Scott, Joshua S. Sapsford, Andrew E. Ashley,\* Gregory G. Wildgoose,\* and J. Chris Slootweg\*

**Abstract:** We herein explore whether tris(aryl)borane Lewis acids are capable of cleaving  $H_2$  outside of the usual Lewis acid/base chemistry described by the concept of frustrated Lewis pairs (FLPs). Instead of a Lewis base we use a chemical reductant to generate stable radical anions of two highly hindered boranes: tris(3,5-dinitromesityl)borane and tris(mesityl)borane. NMR spectroscopic characterization reveals that the corresponding borane radical anions activate (cleave) dihydrogen, whilst EPR spectroscopic characterization, supported by computational analysis, reveals the intermediates along the hydrogen activation pathway. This radical-based, redox pathway involves the homolytic cleavage of  $H_2$ , in contrast to conventional models of FLP chemistry, which invoke a heterolytic cleavage pathway. This represents a new mode of chemical reactivity for hydrogen activation by borane Lewis acids.


The chemistry of Lewis acidic boranes reacting with  $H_2$  is now almost exclusively described by the Lewis acid/base conceptual framework of frustrated Lewis pairs (FLPs),<sup>[1]</sup> introduced by Douglas Stephan in 2006.<sup>[2]</sup> While some precise mechanistic details are still debated,<sup>[3]</sup> in general the ability of


FLPs to cleave  $H_2$  relies on the cooperative action of the two reactive centers that are sterically encumbered (“frustrated”) within an encounter complex of the Lewis acid–base pair. The Lewis acid, which is most often an organoborane, provides a vacant acceptor orbital, and the Lewis base, typically a phosphine or amine, provides a donor orbital with which to cleave the strong H–H bond.<sup>[4]</sup> Activation of  $H_2$  by borane-based FLPs is therefore widely thought to involve heterolytic bond cleavage, and to be controlled by the relative strengths of the Lewis acidic/Lewis basic components and the degree of steric encumbrance between them.<sup>[1b–e,5]</sup> This contrasts with the transition-metal-based complexes and biological systems that have dominated hydrogenation catalysis for the previous 150 years.<sup>[6]</sup> In these complexes, the metal center provides both vacant and filled acceptor/donor orbitals at a single reactive site; the chemistry is, to a large extent, operating under redox control of the metal center, and homolytic  $H_2$  bond cleavage is common.

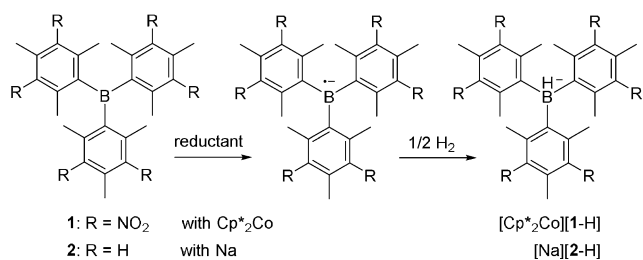
The heterolytic mechanism proposed for FLP activation of  $H_2$  is found generally to be in good agreement with observed trends in reactivity, and it has been supported by a number of computational studies.<sup>[4]</sup> Nevertheless, definitive experimental proof has remained elusive (perhaps unavoidably so). As such it is interesting to consider that observed patterns of FLP reactivity could also be consistent with alternative  $H_2$  activation pathways. These trends could also be consistent with plausible radical mechanisms, in which initial single-electron transfer (SET) from the Lewis base to the Lewis acid would transiently generate highly reactive radical pairs capable of activating  $H_2$ . For example, while the thermodynamic and kinetic ability of an FLP to activate  $H_2$  is well known to correlate with the hydride-ion affinity of the Lewis acid (consistent with heterolytic bond cleavage), these parameters also correlate well with the one-electron reduction potential of the Lewis acid (consistent with SET). Indeed, recent studies have implied that for some families of borane Lewis acids, reduction potentials may even be a better indicator of reactivity towards  $H_2$  than hydride-ion affinities.<sup>[7]</sup>

There is also a growing body of evidence for the occurrence of radical mechanisms when small molecules, such as NO,  $Ph_3SnH$ , and peroxides, are used as the substrates of FLP reactions.<sup>[8]</sup> To date, however, these frustrated radical pair (FRP) mechanisms have not been observed with  $H_2$ . Indeed, no FLP is known to cleave  $H_2$  via a radical mechanism. Our previous work studying the electrochemistry of FLP components, together with the recent evidence for radical pathways in FLPs and FRPs reported by others, raises an obvious question that this article sets out to answer: can

[\*] Dr. E. L. Bennett, Dr. E. J. Lawrence, Dr. R. J. Blagg, A. S. Mullen, Dr. F. MacMillan, Prof. Dr. G. G. Wildgoose  
School of Chemistry, University of East Anglia  
Norwich Research Park, Norwich, NR4 7TJ (UK)  
E-mail: g.wildgoose@uea.ac.uk  
Dr. A. W. Ehlers, Prof. Dr. J. C. Slootweg  
Van 't Hoff Institute for Molecular Sciences, University of Amsterdam  
Science Park 904, PO Box 94157,  
1090 GD Amsterdam (The Netherlands)  
E-mail: j.c.slootweg@uva.nl  
Dr. A. W. Ehlers  
Department of Chemistry, Science Faculty,  
University of Johannesburg  
PO Box 254, Auckland Park, Johannesburg (South Africa)  
Dr. D. J. Scott, J. S. Sapsford, Dr. A. E. Ashley  
Molecular Sciences Research Hub,  
Imperial College White City Campus  
80 Wood Lane, London W12 0BZ (UK)  
E-mail: a.ashley@imperial.ac.uk

 Supporting information and the ORCID identification number(s) for the author(s) of this article can be found under:  
<https://doi.org/10.1002/anie.201900861>.

 © 2019 The Authors. Published by Wiley-VCH Verlag GmbH & Co. KGaA. This is an open access article under the terms of the Creative Commons Attribution Non-Commercial NoDerivs License, which permits use and distribution in any medium, provided the original work is properly cited, the use is non-commercial, and no modifications or adaptations are made.



**Scheme 1.** Reduction of tris(3,5-dinitromesityl)borane **1**, and tris(mesityl)borane **2**, and subsequent reaction with H<sub>2</sub>.

boranes react with H<sub>2</sub> outside of an FLP chemical framework, if they can operate via a hitherto unknown redox controlled, radical reaction pathway instead?

To test our hypothesis, we carefully selected two boranes as models: tris(3,5-dinitromesityl)borane **1**, and tris(mesityl)borane **2** (Scheme 1). Both boranes have essentially identical steric shielding of the central boron atom by the six *ortho* methyl groups on the mesityl rings, leading to the formation of long-lived borane radical anions upon reduction.<sup>[9,10]</sup> Neither borane is currently known to be active for H<sub>2</sub> activation within an FLP. The addition of six electron-withdrawing nitro groups in **1** shifts the reduction potential in a positive direction to  $-1.57$  V vs. Cp<sub>2</sub>Fe<sup>0/+</sup> (see the Supporting Information), making **1** as electrophilic and comparably facile to reduce as the archetypal electron-deficient borane B(C<sub>6</sub>F<sub>5</sub>)<sub>3</sub> used in FLP chemistry ( $-1.52$  V vs. Cp<sub>2</sub>Fe<sup>0/+</sup>),<sup>[7b,e-g]</sup> and much easier to reduce than **2** (approximately  $-2.8$  V vs. Cp<sub>2</sub>Fe<sup>0/+</sup>).<sup>[11]</sup> The NO<sub>2</sub> groups in **1** also provide useful electron paramagnetic resonance spectroscopic markers for the characterization of reaction intermediates.

To examine whether the radical anions of Lewis acidic boranes are capable of cleaving hydrogen, a solution of **1** in either CD<sub>2</sub>Cl<sub>2</sub> or [D<sub>8</sub>]THF was chemically reduced using decamethylcobaltocene (Cp\*<sub>2</sub>Co,  $E^0 = -1.94$  V vs. Cp<sub>2</sub>Fe<sup>0/+</sup>),<sup>[12]</sup> heated in the presence of H<sub>2</sub>, and the reaction periodically monitored using multinuclear NMR spectroscopy (see the Supporting Information for details). Figure 1 a shows the resulting <sup>11</sup>B NMR spectra. The formation of the borohydride product [Cp\*<sub>2</sub>Co][1-H] is clearly evident by the observation of a characteristic doublet at  $\delta = -13.6$  ppm ( $^1J_{\text{B,H}} = 82$  Hz) in the <sup>11</sup>B NMR spectrum and the corresponding 1:1:1:1 quartet at  $\delta = +3.8$  ppm ( $^1J_{\text{H,B}} = 82$  Hz) in the <sup>1</sup>H NMR spectrum. The spectral assignment was further confirmed by comparison to an authentic sample of [Na][1-H] (Supporting Information, Figure S10). Control experiments using D<sub>2</sub> in *protio*-CH<sub>2</sub>Cl<sub>2</sub> or *protio*-THF produced the analogous result, the generation of [Cp\*<sub>2</sub>Co][1-D] (Supporting Information, Figures S11 and S12), observed as a partially resolved triplet at  $\delta = -13.6$  ppm in the <sup>11</sup>B NMR spectrum.

In these reactions, the cleavage of H<sub>2</sub>/D<sub>2</sub> must be homolytic as there is no apparent plausible mechanism to allow for the formation of H<sup>+</sup> (no counter anion), which must be produced via heterolytic scission of H<sub>2</sub>. Whilst very strong acids are known to protonate Cp\*<sub>2</sub>Co,<sup>[13]</sup> there is no observable evidence for the formation of this in these reactions. To examine the proposed radical homolytic dihydrogen cleavage mechanism, **1** was again reduced with Cp\*<sub>2</sub>Co under H<sub>2</sub> but this time in the

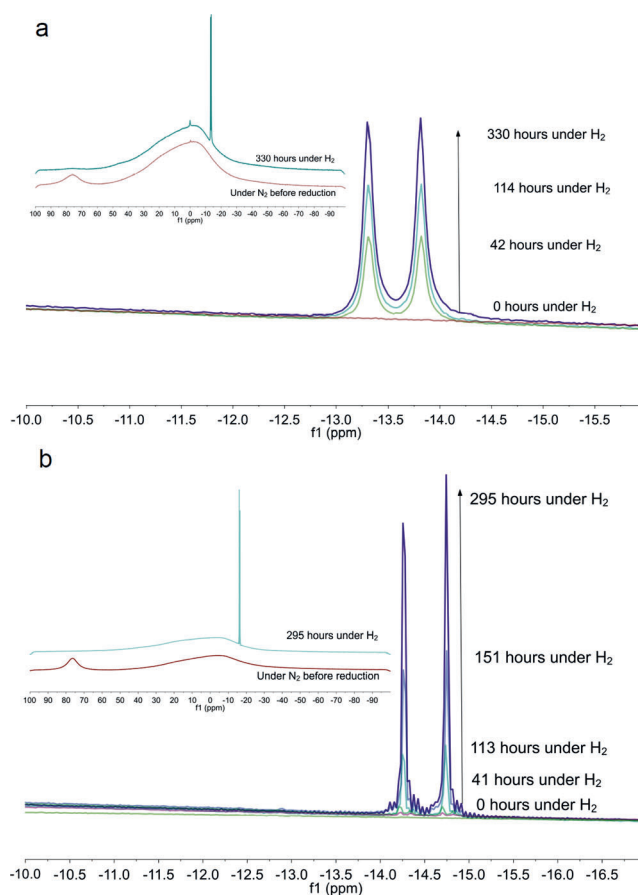


**Figure 1.** Overlaid <sup>11</sup>B NMR spectra expanded over the B–H bond region of interest, showing the progression of H<sub>2</sub> cleavage by chemical reduction of **1** in CD<sub>2</sub>Cl<sub>2</sub> (a) and **2** in THF (b). Inset: The corresponding <sup>11</sup>B NMR spectra recorded at the start and end of the experiments showing the conversion of the parent borane starting material to the borohydride product upon reduction and exposure to H<sub>2</sub>.

presence of 1 equiv of the radical spin-trap TEMPO ((2,2,6,6-tetramethylpiperidin-1-yl)oxyl). TEMPO was selected because it does not coordinate to the bulky borane **1** and has a more negative reduction potential than Cp\*<sub>2</sub>Co,<sup>[14]</sup> thus precluding any possible redox inhibition to form [TEMPO]<sup>−</sup> and **1**, which together could subsequently participate in FLP H<sub>2</sub> activation. In the presence of TEMPO, no H<sub>2</sub> cleavage was observed, consistent with inhibition of a radical reaction by the TEMPO spin-trap. Additional control experiments confirm that Cp\*<sub>2</sub>Co alone does not activate H<sub>2</sub> under these conditions and that THF/**1** mixtures do not result in the observable formation of [1-H]<sup>−</sup> via a solvent-FLP mechanism<sup>[15]</sup> in the absence of a reducing agent. Crucially, no evidence of reduction at the nitro groups is observed by NMR, EPR, nor IR spectroscopic characterization of the reaction products.

The very negative redox potential of **2** necessitates the use of a stronger reducing agent. When a solution of **2** in [D<sub>8</sub>]THF is reduced over sodium metal<sup>[10]</sup> and heated in the presence of H<sub>2</sub> the appearance of a doublet in the <sup>11</sup>B NMR spectrum at  $\delta = -14.5$  ppm ( $^1J_{\text{B,H}} = 78$  Hz), and a corresponding 1:1:1:1 quartet in the <sup>1</sup>H NMR spectrum at  $\delta = 3.75$  ppm ( $^1J_{\text{H,B}} = 77$  Hz) is observed, characteristic of the formation of [Na][2-H] (Figure 1 b).

The experiments described above clearly indicate that the borane radical anions **1**<sup>•−</sup> and **2**<sup>•−</sup> can cleave H<sub>2</sub> in the absence of any exogenous Lewis base. These reactions are, however, slow in comparison to typical FLP H<sub>2</sub> activation reactions. In the case of the model borane **1**, this is advantageous, since it enables the reaction to be monitored in real time and reaction intermediates along the H<sub>2</sub> cleavage pathway to be observed using EPR spectroscopy.

Solutions of **1** dissolved in either CD<sub>2</sub>Cl<sub>2</sub> or [D<sub>8</sub>]THF were chemically reduced using Cp\*<sub>2</sub>Co (see Supporting Information) and the EPR spectra resulting from exposure to H<sub>2</sub> were recorded (Figures 2a–d). Simulation of the EPR spectra yields the isotropic hyperfine coupling constants for the various <sup>1</sup>H, <sup>14</sup>N, and <sup>11</sup>B nuclei, given in Table 1. These data, supported by DFT calculations (performed for the identifiable intermediates of both **1** and **2**, and detailed in the Supporting Information), enable us to observe and characterize the structures of the intermediates and gain valuable insights into the reaction mechanism (given schematically in Figure 3) and the corresponding energetic profile by which organoborane radicals cleave H<sub>2</sub> homolytically (Figure 4).

Upon reduction of **1** under N<sub>2</sub>, the EPR spectrum shown in Figure 2a is observed, which is characteristic of **1**<sup>•−</sup> with

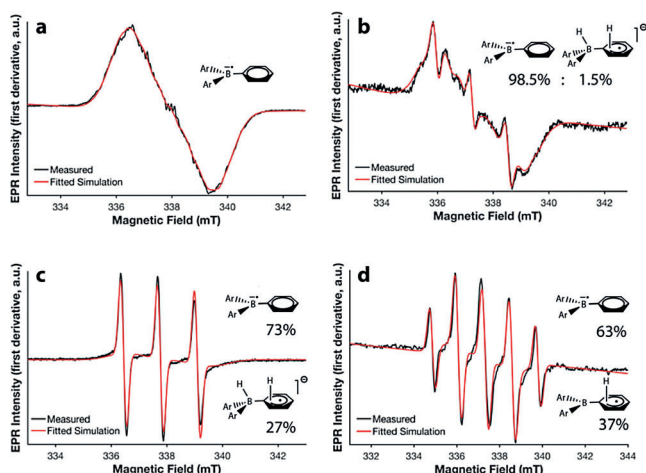


**Figure 2.** EPR spectra of **1**<sup>•−</sup> formed via chemical reduction of **1**, recorded under an atmosphere of N<sub>2</sub> (a), upon first exposure to H<sub>2</sub> but prior to heating (b), after heating under H<sub>2</sub> for 10 minutes (c), and after heating under H<sub>2</sub> for 48 hours (d). The structures of the paramagnetic species are shown with ring substituents removed for clarity.

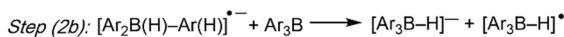
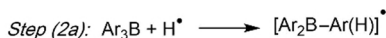
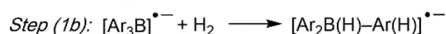
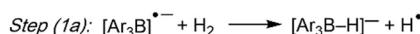
**Table 1:** EPR spectral parameters obtained by simulation of the experimental spectra recorded in Figures 2A–D.

Parameter	Simulated Spectra						
	Figure 2a <b>1</b> <sup>•−</sup>	Figure 2b <b>1</b> <sup>•−</sup>	Figure 2b [ <b>1</b> -{H <sub>2</sub> }] <sup>•−</sup>	Figure 2c <b>1</b> <sup>•−</sup>	Figure 2c [ <b>1</b> -{H <sub>2</sub> }] <sup>•−</sup>	Figure 2d <b>1</b> <sup>•−</sup>	Figure 2d [ <b>1</b> -H] <sup>•</sup>
g-value	2.00475	2.00473	2.00619	2.00473	2.00640	2.00473	2.00404
A ( <sup>11</sup> B)/ MHz	23.2	23.3	–	23.3	–	23.3	35.4
A ( <sup>14</sup> N, meta-NO <sub>2</sub> )/ MHz	3.6	3.4	36.5	3.4	37.3	3.5	0.7
A ( <sup>1</sup> H, ortho-CH <sub>3</sub> )/ MHz	4.8	4.2	–	4.2	–	4.2	0.5
A ( <sup>1</sup> H, para-CH <sub>3</sub> )/ MHz	7.9	7.8	–	7.8	–	7.9	1.8
A ( <sup>1</sup> H)/ MHz	–	–	–	–	–	–	32.2
Linewidth (Gaussian)/ mT	0.15	0.25	0.22	0.25	0.22	0.20	0.26
Weighting	–	98.5 %	1.5 %	73.0 %	27.0 %	63.0 %	37.0 %
RMSD	0.022532	0.038452	–	0.034853	–	0.060845	–

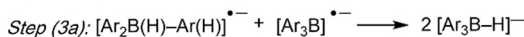
#### Initiation



#### Propagation



#### Termination



#### Termination-Propagation

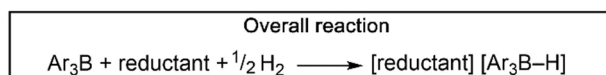
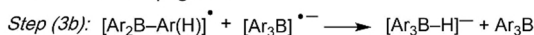


**Figure 3.** The proposed radical chain-propagation mechanism for the homolytic cleavage of H<sub>2</sub> upon reduction of organoborane Lewis acids. Inset: the chemical structures corresponding to the [Ar<sub>2</sub>B(H)-Ar(H)]<sup>•−</sup> and [Ar<sub>2</sub>B-Ar(H)]<sup>•</sup> intermediates (substituents on the aryl rings have been omitted for clarity).

hyperfine coupling of the unpaired electron spin density to the boron nucleus as well as the methyl and nitro substituents on the aromatic rings (Table 1).<sup>[16]</sup> The initiation step is calculated to be exothermic for both compounds (−56.7 and −11.7 kcal mol<sup>−1</sup> for **1** and **2**, respectively) and reflects the relative LUMO energy and reduction potential of each borane.

Figure 2b shows the resulting spectrum recorded upon first exposing the reaction to H<sub>2</sub> and before heating. An immediate change is evident with the appearance of a sharp 1:1:1 three-line signal superimposed on the original signal of the **1**<sup>•−</sup> parent. After heating the reaction for a further 10 minutes this three-line signal dominates the EPR spectral response (Figure 2c) for the next 48 hours. The only change to the system is the addition of H<sub>2</sub> and computational modelling of the possible interactions between **1**<sup>•−</sup> and H<sub>2</sub> reveal two propagation pathways. Propagation 1a produces the diamagnetic borohydride product, and is endothermic (+30.8 and +28.1 kcal mol<sup>−1</sup> for **1** and **2**), albeit to a lesser extent than homolytic H<sub>2</sub> splitting itself (+107.1 kcal mol<sup>−1</sup> at this level of theory). The alternative pathway, Propagation 1b avoids the

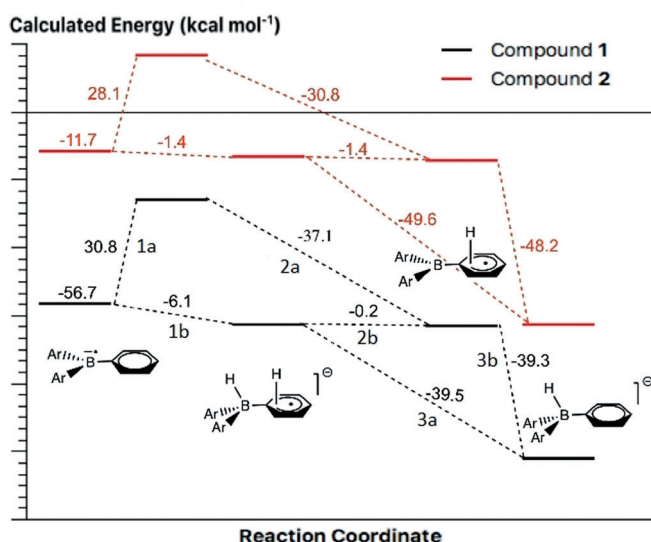


**Figure 4.** Postulated reaction profile showing the relevant reaction intermediates involved in each step (ring substituents removed for clarity, steps labeled as in Figure 3) together with the associated change in energy values along each reaction step obtained from DFT calculations.

release of free H-atom radicals and is slightly exothermic ( $-6.1$  and  $-1.4$  kcal mol $^{-1}$  for **1** and **2**). This reaction produces a radical species consistent with that observed in Figures 2b,c. Computation reveals the structure of this intermediate to be  $[(\text{Ar}_2\text{B}(\text{H})-\text{Ar}(\text{H}))^\bullet]^-$  with hydride attached at a four-coordinate boron centre, and H $^\bullet$  carried on one of the aromatic rings (denoted as  $[\mathbf{1}\text{-}\{\text{H}_2\}]^\bullet$  with specific reference to borane **1**). DFT models indicate that there is little energetic discrimination for the H $^\bullet$  to be attached to one or other carbon positions around the aromatic ring. Spin-density calculations (see Data S1 in the Supporting Information) confirm, however, that the isomer with the H $^\bullet$  predominantly located at a *meta* carbon on the ring, *ipso* to one of the nitro groups, is consistent with the observed EPR spectra (Figures 2b,c). Here the unpaired electron is coupled only to one of the nitrogen nuclei in the nitro groups of the aryl ring system and is not coupled to the boron nucleus at all (Table 1).

After 48 hours of heating, the EPR spectrum changes once again (Figure 2d) to reveal a 1:2:2:2:1 five-line hyperfine coupling pattern of a new persistent paramagnetic species. This does not fit the expected coupling pattern from two nitro groups which would give rise to a 1:2:3:2:1 splitting pattern. Instead, it arises from near coincident hyperfine coupling with both an additional single hydrogen atom and the boron nucleus (similar to DFT calculations of a hydrogen-boron adduct).<sup>[17]</sup> This is a neutral  $[\mathbf{1}\text{-H}]^\bullet$  intermediate resulting from cleavage of the H $_2$  molecule.

Once again there are two possible pathways that result in the formation of the  $[\mathbf{1}\text{-H}]^\bullet$  intermediate: Propagation 2a and Propagation 2b. Propagation 2a is exothermic by  $-37.1$  kcal mol $^{-1}$  and  $-30.8$  kcal mol $^{-1}$  for **1** and **2**, respectively. Interestingly, computation suggests that if  $[\mathbf{1}\text{-H}]^\bullet$  is formed with the hydrogen atom at boron, as one might expect, the hydrogen atom immediately hops from the boron atom onto the aromatic ring system, until it arrives at the *para* carbon

atom which is the most stable isomer in the case of **1** (whereas the *meta* position is most stable in **2**, see Table S1 in the Supporting Information). This is supported by what is observed experimentally during the EPR spectroscopic monitoring of hydrogen splitting by **1** where the magnitude of the resulting H $^\bullet$  atom hyperfine coupling fits well with coupling to spin density on the ring system in the *para* position located between the two nitro groups (Figure 2d).

If the parent borane is present in excess of the radical anion (Propagation 2b), the hydrogen atom produced in step 1a (considered as  $[\text{Ar}_2\text{B}(\text{H})-\text{Ar}(\text{H}))^\bullet]^-$ ) may be transferred, and the borohydride product and the neutral  $[\text{Ar}_3\text{B}-\text{H}]^\bullet$  radical intermediate formed. Using the values calculated for propagation steps 1a and 2a, step 2b is energetically neutral. In the system reported herein, it is unlikely that the parent borane is present in excess of the radical anion initially, but as the reaction proceeds through step 3b and the consumption of the  $[\text{Ar}_2\text{B}(\text{H})-\text{Ar}(\text{H}))^\bullet]^-$  progresses, this stabilization may become more relevant towards the end of the reaction. This situation may also have relevance to potential radical-FLP hydrogen cleavage mechanisms, where the parent borane is most likely present in excess of any potential radical anion intermediates throughout.

The final step in the reaction, which cannot be observed by EPR spectroscopy, is the formation of the diamagnetic  $[\mathbf{1}\text{-H}]^-$  product, which is detected by  $^{11}\text{B}$  and  $^1\text{H}$  NMR spectroscopic analysis of the reaction mixture at the end of the experiment. Aside from the obvious recombination of 2H $^\bullet$  to form H $_2$  (the reverse of step 1), there are two termination pathways: Termination 3a ( $-39.5$  and  $-49.6$  kcal mol $^{-1}$  for **1** and **2**, respectively), and Termination-Propagation 3b ( $-39.3$  and  $-48.2$  kcal mol $^{-1}$  for **1** and **2**, respectively). Step 3a may also be written as  $[\text{Ar}_3\text{B}]^\bullet + \text{H}^\bullet \rightarrow [\text{Ar}_3\text{B}-\text{H}]^-$  for consistency with the rest of the Scheme, or as a termolecular reaction:  $2[\text{Ar}_3\text{B}]^\bullet + \text{H}_2 \rightarrow 2[\text{Ar}_3\text{B}-\text{H}]^-$ . Step 3b yields both the terminal borohydride product and regenerates the parent neutral borane for further reaction in propagation step 2a. Note that whilst it would appear from Figures 2c,d that the EPR spectra are dominated by the  $[\mathbf{1}\text{-}\{\text{H}_2\}]^\bullet$  and  $[\mathbf{1}\text{-H}]^\bullet$  species, respectively, simulation of the spectral data reveals that these spectra are each superimposed over the parent  $\mathbf{1}^\bullet$  radical anion species. As the reaction proceeds with heating the weighting between the systems changes ( $\mathbf{1}^\bullet$  :  $[\mathbf{1}\text{-}\{\text{H}_2\}]^\bullet = 98.5:1.5$  in Figure 2b;  $73.0:27.0$  in Figure 2c, and  $\mathbf{1}^\bullet$  :  $[\mathbf{1}\text{-H}]^\bullet = 63.0:37.0$  in Figure 2d). The rate of consumption of  $\mathbf{1}^\bullet$  as measured by EPR (Figures 2a–d) correlates with the rate of conversion to borohydride as measured by NMR spectroscopy (Figure 1a).

In summary, using two model boranes, which produce stable radical anions upon one-electron reduction, we have successfully demonstrated homolytic dihydrogen cleavage in the absence of a Lewis base. This represents a new mode of chemical reactivity by Lewis acidic boranes towards H $_2$  that opens up new borane, and potentially other main group chemistries, beyond the framework of conventional FLPs. The reaction between the model borane radical anions and H $_2$  is slow, and the intermediates are sufficiently stabilized so that we can observe several distinct intermediates along the homolytic dihydrogen cleavage pathway using EPR spectroscopy.

copy and can model the energetics of the reaction pathway computationally. We are currently exploring the application of boryl radical  $H_2$  activation as a convenient route to more active borane hydride species, which may have applications in catalysis and energy materials.

## Acknowledgements

The research leading to these results has received funding from the European Research Council under the ERC Grant Agreement no. 307061 (PiHOMER). G.G.W. and A.E.A. thank the Royal Society for financial support via University Research Fellowships (UF/130336 and UF/160395 respectively). F.M. thanks the Royal Society for support via a Wolfson Research Merit Award. A.M. acknowledges the faculties of Science and Medicine at the UEA for funding a PhD studentship. J.C.S. acknowledges the Council for Chemical Sciences of The Netherlands Organization for Scientific Research (NWO/CW) for a VIDI grant (723.012.101). We acknowledge the use of the EPSRC funded National Chemical Database Service hosted by the Royal Society of Chemistry, and the EPSRC UK National Mass Spectrometry Facility (NMSF) at the University of Swansea. We thank the EPSRC UK National Crystallography Service at the University of Southampton for the collection of the crystallographic data.

## Conflict of interest

The authors declare no conflict of interest.

**Keywords:** boranes · dihydrogen · electron paramagnetic resonance · Lewis acids · radicals

- [1] a) J. R. Lawson, R. L. Melen, *Inorg. Chem.* **2017**, *56*, 8627–8643; b) D. W. Stephan, *Science* **2016**, *354*, aaf7229; c) D. W. Stephan, *J. Am. Chem. Soc.* **2015**, *137*, 10018–10032; d) D. W. Stephan, G. Erker, *Angew. Chem. Int. Ed.* **2015**, *54*, 6400–6441; *Angew. Chem.* **2015**, *127*, 6498–6541; e) D. W. Stephan, *Acc. Chem. Res.* **2015**, *48*, 306–316.
- [2] G. C. Welch, R. R. S. Juan, J. D. Masuda, D. W. Stephan, *Science* **2006**, *314*, 1124–1126.
- [3] a) J. Paradies, *Eur. J. Org. Chem.* **2019**, 283–294; b) D. J. Scott, M. J. Fuchter, A. E. Ashley, *Chem. Soc. Rev.* **2017**, *46*, 5689–5700.
- [4] a) G. Skara, F. De Vleeschouwer, P. Geerlings, F. De Proft, B. Pinter, *Sci. Rep.* **2017**, *7*, 1–15; b) T. A. Rokob, I. Papai, *Top. Curr. Chem.* **2013**, *332*, 157–212; c) T. A. Rokob, A. Hamza, A. Stirling, T. Soos, I. Papai, *Angew. Chem. Int. Ed.* **2008**, *47*, 2435–2438; *Angew. Chem.* **2008**, *120*, 2469–2472.
- [5] A. Y. Houghton, T. Autrey, *J. Phys. Chem. A* **2017**, *121*, 8785–8790.
- [6] a) H.-U. Blaser, *Top. Catal.* **2010**, *53*, 997–1001; b) J. Halpern, *Adv. Catal.* **1959**, *11*, 301–370.
- [7] a) R. J. Blagg, E. J. Lawrence, K. Resner, V. S. Oganessian, T. J. Herrington, A. E. Ashley, G. G. Wildgoose, *Dalton Trans.* **2016**, *45*, 6023–6031; b) R. J. Blagg, T. R. Simmons, G. R. Hatton, J. M. Courtney, E. L. Bennett, E. J. Lawrence, G. G. Wildgoose, *Dalton Trans.* **2016**, *45*, 6032–6043; c) R. J. Blagg, G. G. Wildgoose, *RSC Adv.* **2016**, *6*, 42421–42427; d) E. J. Lawrence, T. J. Herrington, A. E. Ashley, G. G. Wildgoose, *Angew. Chem. Int. Ed.* **2014**, *53*, 9922–9925; *Angew. Chem.* **2014**, *126*, 10080–10083; e) E. J. Lawrence, V. S. Oganessian, D. L. Hughes, A. E. Ashley, G. G. Wildgoose, *J. Am. Chem. Soc.* **2014**, *136*, 6031–6036; f) E. J. Lawrence, V. S. Oganessian, G. G. Wildgoose, A. E. Ashley, *Dalton Trans.* **2013**, *42*, 782–789; g) A. E. Ashley, T. J. Herrington, G. G. Wildgoose, H. Zaher, A. L. Thompson, N. H. Rees, T. Krämer, D. O'Hare, *J. Am. Chem. Soc.* **2011**, *133*, 14727–14740.
- [8] a) A. Merk, H. Großekappenberg, M. Schmidtman, M.-P. Luecke, C. Lorent, M. Driess, M. Oestreich, H. F. T. Klare, T. Müller, *Angew. Chem. Int. Ed.* **2018**, *57*, 15267–15271; *Angew. Chem.* **2018**, *130*, 15487–15492; b) L. L. Liu, L. L. Cao, D. Zhu, J. Zhou, D. W. Stephan, *Chem. Commun.* **2018**, *54*, 7431–7434; c) L. L. Liu, L. L. Cao, Y. Shao, G. Ménard, D. W. Stephan, *Chem* **2017**, *3*, 259–267; d) L. L. Liu, L. L. Cao, Y. Shao, D. W. Stephan, *J. Am. Chem. Soc.* **2017**, *139*, 10062–10071; e) L. E. Longobardi, L. L. Liu, S. Grimme, D. W. Stephan, *J. Am. Chem. Soc.* **2016**, *138*, 2500–2503; f) X. Tao, G. Kehr, X. Wang, C. G. Daniliuc, S. Grimme, G. Erker, *Chem. Eur. J.* **2016**, *22*, 9504–9507; g) M. de Oliveira, Jr., T. Wiegand, L.-M. Elmer, M. Sajid, G. Kehr, G. Erker, C. J. Magon, H. Eckert, *J. Chem. Phys.* **2015**, *142*, 124201.
- [9] a) R. Feng, L. Zhang, C. Chen, Y. Fang, Y. Zhao, G. Tan, X. Wang, *Chem. Eur. J.* **2019**, *25*, 4031–4035; b) N. Yuan, W. Wang, Z. Wu, S. Chen, G. Tan, Y. Sui, X. Wang, J. Jiang, P. P. Power, *Chem. Commun.* **2016**, *52*, 12714–12716.
- [10] For a review on radicals derived from Lewis acid/base pairs, see: a) L. L. Liu, D. W. Stephan, *Chem. Soc. Rev.* **2019**, <https://doi.org/10.1039/c8cs00940f>; For the synthesis of borane radical anions, see: b) T. Kawamoto, S. Uehara, H. Hirao, T. Fukuyama, H. Matsubara, I. Ryu, *J. Org. Chem.* **2014**, *79*, 3999–4007; c) T. Kushida, S. Yamaguchi, *Organometallics* **2013**, *32*, 6654–6657; d) P. P. Power, *Chem. Rev.* **2003**, *103*, 789–810 and references therein; e) M. M. Olmstead, P. P. Power, *J. Am. Chem. Soc.* **1986**, *108*, 4235–4236 and references therein.
- [11] S. A. Cummings, M. Imura, C. J. Harlan, R. J. Kwaan, I. Vu Trieu, J. R. Norton, B. M. Bridgewater, F. Jäkle, A. Sundaraman, M. Tilset, *Organometallics* **2006**, *25*, 1565–1568.
- [12] For the reaction of the radical anion  $[B(C_6F_5)_2]^-$  with  $N_2O$ , see: Y. Liu, E. Solari, R. Scopelliti, F. F. Tirani, K. Severin, *Chem. Eur. J.* **2018**, *24*, 18809–18815.
- [13] a) M. J. Chalkley, T. J. Del Castillo, B. D. Matson, J. C. Peters, *J. Am. Chem. Soc.* **2018**, *140*, 6122–6129; b) M. J. Chalkley, T. J. Del Castillo, B. D. Matson, J. P. Roddy, J. C. Peters, *ACS Cent. Sci.* **2017**, *3*, 217–223.
- [14] J. L. Hodgson, M. Namazian, S. E. Bottle, M. L. Coote, *J. Phys. Chem. A* **2007**, *111*, 13595–13605.
- [15] a) T. Mahdi, D. W. Stephan, *J. Am. Chem. Soc.* **2014**, *136*, 15809–15812; b) D. J. Scott, M. J. Fuchter, A. E. Ashley, *J. Am. Chem. Soc.* **2014**, *136*, 15813–15816; c) D. J. Scott, M. J. Fuchter, A. E. Ashley, *Angew. Chem. Int. Ed.* **2014**, *53*, 10218–10222; *Angew. Chem.* **2014**, *126*, 10382–10386.
- [16] a) R. J. Kwaan, C. J. Harlan, J. R. Norton, *Organometallics* **2001**, *20*, 3818–3820; b) C. Elschenbroich, P. Kuhlkamp, A. Behrendt, K. Harms, *Chem. Ber.* **1996**, *129*, 859–869; c) T. J. DuPont, J. L. Mills, *J. Am. Chem. Soc.* **1975**, *97*, 6375–6382.
- [17] J. C. Walton, M. M. Brahmī, J. Monot, L. Fensterbank, M. Malacria, D. P. Curran, E. Lacôte, *J. Am. Chem. Soc.* **2011**, *133*, 10312–10321.

Manuscript received: January 22, 2019

Revised manuscript received: April 9, 2019

Accepted manuscript online: April 9, 2019

Version of record online: ■■■■■■

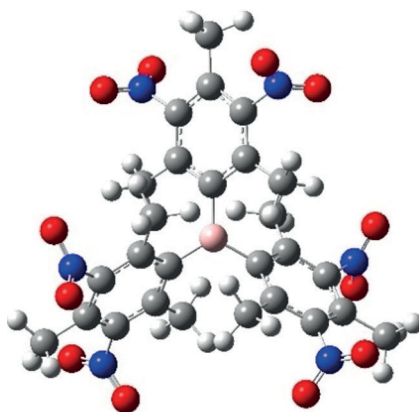
## Communications



## Hydrogen Activation

E. L. Bennett, E. J. Lawrence, R. J. Blagg,  
A. S. Mullen, F. MacMillan, A. W. Ehlers,  
D. J. Scott, J. S. Sapsford, A. E. Ashley,\*  
G. G. Wildgoose,\*  
J. C. Slootweg\* ————— ■■■■-■■■■

A New Mode of Chemical Reactivity for  
Metal-Free Hydrogen Activation by Lewis  
Acidic Boranes



If Lewis acidic boranes, similar to those used in frustrated Lewis pair (FLP) chemistry, are exposed to H<sub>2</sub> in the presence of common reducing agents, instead of the Lewis bases required in FLP chemistry, then homolytic H<sub>2</sub> cleavage occurs. A series of intermediates formed during the H<sub>2</sub> cleavage process at a main group borane complex could be experimentally observed and structurally characterized.